ChemComm

RSC Publishing

COMMUNICATION

View Article Online
View Journal | View Issue

Cite this: *Chem. Commun.*, 2013, **49**, 2679

Received 23rd January 2013,
Accepted 13th February 2013

DOI: 10.1039/c3cc40566d

www.rsc.org/chemcomm

Morphology and phase controlled cobalt nanostructures in magnetic polypropylene nanocomposites: the role of alkyl chain-length in maleic anhydride grafted polypropylene†

Qingliang He,[ab] Tingting Yuan,[a] Zhiping Luo,[c] Neel Haldolaarachchige,[d] David P. Young,[d] Suying Wei*[b] and Zhanhu Guo*[a]

A novel function of maleic anhydride grafted polypropylene (PP) with different backbone chain-lengths was demonstrated, *i.e.*, in controlling the cobalt morphologies (dispersed polyhedral *vs.* assembled chain nanostructure), crystalline structures (ε- *vs.* β-phase), and magnetic property (242 *vs.* 808 Oe) in the synthesized magnetic PP nanocomposites.

Nanoscale cobalt (Co) based materials have shown great potential applications in information data storage, energy storage, catalysis and biomedical areas owing to their unique chemical, structural, magnetic, electronic, and catalytic properties.[1–5] Metallic Co has three crystal structures, *i.e.*, the hexagonal close packed (hcp) α-phase,[6–8] the face centered cubic (fcc) β-phase,[9,10] and a primitive (or pseudo-) cubic ε-phase.[7,11–14] Both hcp- and fcc-Co phases are long-known[15] and the only crystalline structure difference is the stacking sequence of the atomic plane in the (111) direction.[11] Thus, their coexistence is usually observed through high temperature approaches such as melting–crystallization and evaporation–condensation due to the low energy required for stacking fault formation.[11,16] The relatively low temperature solution chemistry such as reduction of cobalt salt[12] and thermal decomposition of organic cobalt precursors[1,7,11,17] has been proved to be ideal for yielding one phase Co.[11] Meanwhile, the hcp structure is more stable at room temperature, while the fcc structure is thermodynamically preferred at above 450 °C.[18] The ε-Co phase was first reported from solution synthesis in 1999.[11,12] The low temperature thermal decomposition or the salt reduction method using a hot injection process can yield temporally separated nucleation and crystal growth,[1] in which Co nanocrystals (NCs) with desired crystal structure can be targeted by facilitating the growth control of selective crystal faults in the presence of different amounts and/or types of surfactant(s).[11,12] Surfactants can also stabilize Co NCs against severe agglomerations arising from the strong van der Waals attractions and the magnetic dipolar interactions. The commonly used surfactants including oleic acid, trioctylphosphine and its oxide, and amines, however, were reported to synthesize Co NCs only at the milligram level. Unfortunately, the preparation of at least gram-level Co NCs with controllable crystal phase, morphology and corresponding physicochemical properties has not been reported. By using a conventional plastic additive, maleic anhydride grafted polypropylene (MA-g-PP), as a novel surfactant to stabilize Co NCs, we demonstrate a unique function of MA-g-PP to control the particle morphology, crystal phase and magnetic property during the preparation of large-scale magnetic PP–Co polymer nanocomposites (PNCs). Specifically, by varying the MA-g-PP backbone length, self-assembled chain structured β-Co spherical NCs and well dispersed highly crystalline polyhedral shaped ε-Co NCs were prepared on a 10 gram scale. Briefly, PP–Co PNCs were prepared using a typical wet chemistry method by injecting dicobalt octacarbonyl ($Co_2(CO)_8$) into a refluxing PP/xylene solution in the presence of MA-g-PP. The PP–Co PNCs in the absence of MA-g-PP were also prepared for comparison.

For PP–Co PNCs, the black composite powders were observed to be highly susceptible to a small magnet, indicating the existence of metallic Co. The transmission electron microscopy (TEM) image, Fig. 1(a), shows the presence of ~24.1 nm roughly spherical Co NCs (without MA-g-PP) with a broad size distribution (~22% standard deviation in diameter). The Co NCs were partially assembled into chain-like structure with some agglomeration. A closer observation of the high-resolution TEM (HRTEM) image, Fig. 1(b), demonstrated a dark core and light shell structure for the typical Co NCs. Moreover, the strong ring patterns in the selected area electron diffraction (SAED), Fig. S1a (refer to ESI†), can be assigned to the (111), (200), (220) and (222) planes of fcc-Co (PDF# 15-0806), while the other two rings are indexed to (102) and (203) planes of Co_2O_3 (PDF# 02-0770). The metallic Co core–Co_2O_3 shell observations are also supported by

[a] *Integrated Composites Laboratory (ICL), Dan F. Smith Department of Chemical Engineering, Lamar University, Beaumont, Texas 77710, USA. E-mail: zhanhu.guo@lamar.edu; Tel: +1 409 880 7654*

[b] *Department of Chemistry and Biochemistry, Lamar University, Beaumont, Texas 77710, USA. E-mail: suying.wei@lamar.edu; Tel: +1 409 880 7976*

[c] *Department of Chemistry and Physics and Southeastern North Carolina Regional Microanalytical and Imaging Consortium, Fayetteville State University, Fayetteville, NC 28301, USA*

[d] *Department of Physics and Astronomy, Louisiana State University, Baton Rouge, Louisiana 70803, USA*

† Electronic supplementary information (ESI) available: Experimental details, additional information including all types of data. See DOI: 10.1039/c3cc40566d

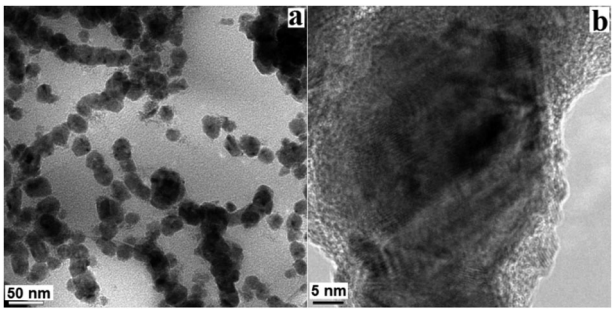

Fig. 1 (a) TEM and (b) HRTEM images of PP–20.0% Co PNCs.

the X-ray diffraction (XRD) study, Fig. S1b (ESI†), where the strongest peak at 44.2° corresponds to the metallic fcc-Co (111) plane and the less intensive peak at lower position (2θ of 38.6°) can be assigned to the (102) plane of Co_2O_3 (PDF# 02-0770). The similar peak intensity between Co_2O_3 and Co (Fig. S1b, ESI,† ratio of ~4 : 5) indicates that a severe oxidation takes place when these Co NCs are not stabilized by any MA-g-PP. It should be emphasized that the freshly synthesized PP–Co PNCs are vulnerable to oxidization under air conditions. Thus, a layer of Co_2O_3 formed on the surface of these Co NCs and appeared to passivate the particle surface and against their further oxidation.[11] This passivation agrees well with our recent observation in Fe NCs.[19]

The addition of 5.0 wt% long chain MA-g-PP (M_n = 2500) to the PP–20.0% Co system leads to a decreased particle size (average size: ~22.4 nm, and size distribution standard deviation: ~20%) with a combination of Co NC chains and individual NCs, Fig. 2(a). Apparently, the decreased particle size is attributed to the particle growth impeded by MA-g-PP. The Co core and oxide shell structure is also observed, Fig. 2(b). The strong ring patterns in the SAED pattern (Fig. S2a, ESI†) can be assigned to the (111), (200), (220), and (311) planes of fcc-Co (PDF# 15-0806). Meanwhile, another ring pattern overlapped with the (111) plane of fcc-Co can be assigned to the (102) plane of Co_2O_3 (PDF# 02-0770). The less oxidization on the Co surface with the addition of MA-g-PP indicated by SAED patterns is further confirmed by the XRD observation (Fig. S2b, ESI†) with a significantly suppressed peak in the (102) plane of Co_2O_3 (2θ = 38.6°) accompanied by a strong metal fcc-Co (111) peak at 2θ of 44.2° (peak intensity ratio of Co_2O_3–Co is ~1 : 5). Thus, MA-g-PP must have a significant passivation on the as-synthesized Co NCs, effectively preventing them from oxidation. Similar to carboxylic acid, maleic anhydride groups in MA-g-PP can react with trace moisture in xylene, resulting in two carboxylic groups, which are excellent stabilizers binding on the Co NCs.[12,20]

When the long chain MA-g-PP was replaced with a short chain MA-g-PP (M_n = 800), XRD study (Fig. S3, ESI†) showed a unique crystal structure of the Co NCs formed in the resulting PP–5.0% MA-g-PP–20.0% Co PNCs exhibiting three intense diffraction peaks at 2θ of 44.6, 47.0, and 49.5°. The positions of these three peaks and their intensity ratios fit well with the reported ε-phase Co,[11] which has a unit cell similar to high temperature β-phase manganese with a cubic structure (space group $P4_132$).[21–23] With less nearest atoms than the ideal close-packed structure, the ε-Co is less condensed than both the hcp- and fcc-ones. Due to the noisy background of the XRD curve, there are barely any additional peaks to be indexed except several weak diffraction peaks at 2θ of ~60°. The Co NCs were observed to have uniform dispersion, Fig. 3(a), which is different from the morphology formed in the presence of long chain MA-g-PP (M_n = 2500). The average size is 40.8 nm with ~11% standard deviation. HRTEM images, Fig. 3(b) and (c), have further identified the anisotropic polyhedral shapes for individual Co NCs. Specifically, hexagonal, rhombic, and cubic shapes were observed consistent with the reported ε-phase Co NCs (rhombic dodecahedron structure shown in Scheme S2, ESI†) with assembly on the 2-D surface from polyhedron shapes projected along the [62$\bar{5}$], [120], and [001] direction, respectively.[24] This has demonstrated that the Co crystal structure can be controlled using MA-g-PP with different alkyl chain lengths. The short MA-g-PP chains give more bonding density on the surface of Co NCs, which leads to dispersed large NC assembly. The detailed Co nanostructure evolutions with different crystal phase and assembly morphology are described in the ESI.†

Fig. 4 shows the room temperature hysteresis loops of the as-prepared PP–Co PNCs in the presence and absence of MA-g-PP and the data are listed in Table S1 (ESI†). The saturation

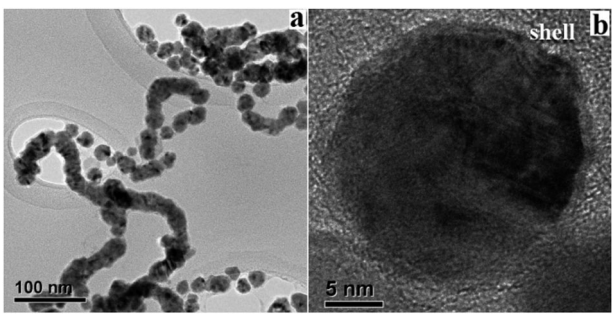

Fig. 2 (a) TEM and (b) HRTEM of PP–20.0% Co PNCs with 5.0% MA-g-PP (M_n = 2500).

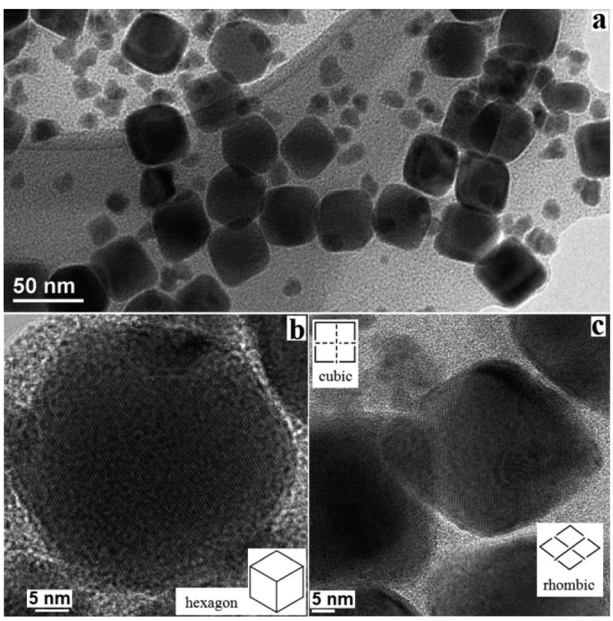

Fig. 3 (a) TEM, (b) and (c) HRTEM of PP–20.0% Co PNCs with 5.0% MA-g-PP (M_n = 800).

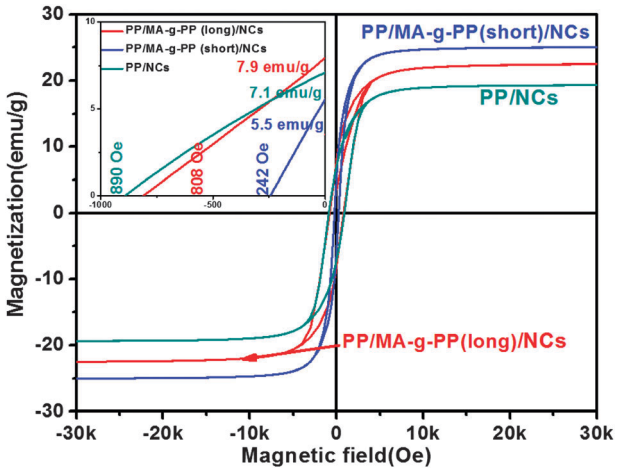

Fig. 4 Room temperature magnetic hysteresis loops of the PP–20.0% Co PNCs with or without 5.0% MA-g-PP.

magnetization (M_s) was observed to increase significantly when adding 5.0% MA-g-PP (short or long chain) to PP–20.0% Co PNCs, *i.e.*, M_s increased from 19.5 (PP–20.0% Co PNCs) to 25.2 emu g^{-1} composite when 5.0% short chain MA-g-PP was used. The M_s of all the three PP PNCs was found to be lower than that of the bulk Co ($\sim$162–166 emu g^{-1}) based on pure Co species (refer to ESI,† Table S1), indicating the existence of an anti-ferromagnetic cobalt oxide layer formed on the Co NC surface. However, the increased magnetization in the presence of MA-g-PP suggests that the chemical bonding between the MA groups and the Co_2O_3 layer enhanced the anti-oxidization strength, so that the Co surface can be passivated with less oxide formation, which in turn leads to a stronger magnetization. In addition, the stronger M_s obtained using short chain MA-g-PP than that obtained using its long chain counterpart is primarily attributed to higher passivation intensity derived from higher bonding density between carboxylic groups and Co NCs. The low molecular weight MA-g-PP has more MA groups, which give a higher bonding density and lead to a stronger stability of the formed Co NCs against oxidation.[12] This is also consistent with our recent observation in the Fe NCs.[19] Meanwhile, the atomic magnetic moment in ε-Co is slightly lower than that of bulk α- and β-Co,[11] which further intensifies the passivation effect of the short alkyl chain MA-g-PP. In addition, the coercive forces (H_c) were all higher than 200 Oe, indicating hard ferromagnetic behaviour of all the PP PNCs. However, H_c decreased drastically from 890 Oe for PP–20.0% Co PNCs to 242 Oe for PP–20.0% Co–5.0% MA-g-PP (M_n = 800) PNCs. In general, fcc-Co is a soft magnet compared to hcp-Co.[5,25] Thus, the high H_c of both PP–20.0% Co and PP–5.0% MA-g-PP (M_n = 2500)–20.0% Co PNCs are attributed to strong shape anisotropy from these nanochains formed by fcc-Co NCs and exchange coupling between the ferromagnetic Co core and the anti-ferromagnetic Co_2O_3 shell.[26] Usually, single domain Co NCs with a reported critical domain size of $\sim$70 nm have a low H_c less than 100 Oe.[9] The relatively high H_c observed in the PP–5.0% MA-g-PP (M_n = 800)–20.0% Co PNCs (242 Oe) is primarily attributed to the exchange coupling between the Co core and the Co_2O_3 shell with a minor effect from shape anisotropy due to the lack of chain structure.

In summary, a new function of the long-known plastic additive, MA-g-PP, to manipulate the Co NC morphology, crystal structure and magnetic property in synthesizing large-scale magnetic PP–Co PNCs by only changing the chain length of MA-g-PP has been successfully demonstrated. The merits of this method including low-temperature, large-scale, one-pot route and structure compatibility with many kinds of polyolefin plastics will broaden the utilization of MA-g-PP in preparing magnetic plastic-based PNCs with desirable applications.

This project is supported by the Research Enhancement Grant from Lamar University. Partial support from NSF under grant No. CBET 11-37441 and CMMI 10-30755 and that from Baker Hughes Inc. are appreciated. D. P. Young acknowledges support from the NSF under Grant No. DMR 10-05764.

Notes and references

1 (*a*) V. F. Puntes, K. M. Krishnan and A. P. Alivisatos, *Science*, 2001, **291**, 2115–2117; (*b*) S. Wei, Q. Wang, J. Zhu, L. Sun and Z. Guo, *Nanoscale*, 2011, **3**, 4474–4502.
2 H. Shao, Y. Huang, H. S. Lee, Y. J. Suh and C. O. Kim, *J. Appl. Phys.*, 2006, **99**, 08N702-708N702-703.
3 (*a*) Z. Guo, C. Kumar, L. Henry, E. E. Doomes, J. Hormes and E. Podlaha, *J. Electrochem. Soc.*, 2005, **152**(1), D1–D5; (*b*) Z. Guo, M. Moldovan, D. P. Young, L. L. Henry and E. J. Podlaha, *Electrochem. Solid-State Lett.*, 2007, **10**, E31–E35; (*c*) I. de PR Moreira, A. Roldán and F. Illas, *J. Chem. Phys.*, 2010, **133**, 024701.
4 D. H. Ha, M. A. Islam and R. D. Robinson, *Nano Lett.*, 2012, **12**, 5122–5130.
5 C. Osorio-Cantillo, A. Santiago-Miranda, O. Perales-Perez and Y. Xin, *J. Appl. Phys.*, 2012, **111**, 07B324-307B324-323.
6 H. Sato, O. Kitakami, T. Sakurai, Y. Shimada, Y. Otani and K. Fukamichi, *J. Appl. Phys.*, 1997, **81**, 1858–1862.
7 V. F. Puntes, D. Zanchet, C. K. Erdonmez and A. P. Alivisatos, *J. Am. Chem. Soc.*, 2002, **124**, 12874–12880.
8 F. S. Diana, S. H. Lee, P. M. Petroff and E. J. Kramer, *Nano Lett.*, 2003, **3**, 891–895.
9 R. N. Grass and W. J. Stark, *J. Mater. Chem.*, 2006, **16**, 1825–1830.
10 K. M. Nam, J. H. Shim, H. Ki, S.-I. Choi, G. Lee, J. K. Jang, Y. Jo, M.-H. Jung, H. Song and J. T. Park, *Angew. Chem., Int. Ed.*, 2008, **47**, 9504–9508.
11 D. P. Dinega and M. G. Bawendi, *Angew. Chem., Int. Ed.*, 1999, **38**, 1788–1791.
12 S. Sun and C. Murray, *J. Appl. Phys.*, 1999, **85**, 4325–4330.
13 Z. Zhou, G. Liu and D. Han, *ACS Nano*, 2009, **3**, 165–172.
14 Y. Bao, W. An, C. H. Turner and K. M. Krishnan, *Langmuir*, 2010, **26**, 478–483.
15 A. W. Hull, *Phys. Rev.*, 1921, **17**, 571–588.
16 L. Hofer and W. Peebles, *J. Am. Chem. Soc.*, 1947, **69**, 893–899.
17 Y. Yin, R. M. Rioux, C. K. Erdonmez, S. Hughes, G. A. Somorjai and A. P. Alivisatos, *Science*, 2004, **304**, 711–714.
18 O. Kitakami, H. Sato, Y. Shimada, F. Sato and M. Tanaka, *Phys. Rev. B*, 1997, **56**, 13849–13854.
19 (*a*) J. Zhu, Q. He, Z. Luo, A. Khasanov, Y. Li, L. Sun, Q. Wang, S. Wei and Z. Guo, *J. Mater. Chem.*, 2012, **22**, 15928–15938; (*b*) J. Zhu, S. Wei, Y. Li, L. Sun, N. Haldolaarachchige, D. Young, C. Southworth, A. Khasanov, Z. Luo and Z. Guo, *Macromolecules*, 2011, **44**, 4382–4391.
20 Q. He, T. Yuan, S. Wei, N. Haldolaarachchige, Z. Luo, D. P. Young, A. Khasanov and Z. Guo, *Angew. Chem., Int. Ed.*, 2012, **51**, 8842–8845.
21 V. F. Puntes, K. M. Krishnan and P. Alivisatos, *Appl. Phys. Lett.*, 2001, **78**, 2187–2189.
22 M. O'Keeffe and S. Andersson, *Acta Crystallogr., Sect. A: Cryst. Phys., Diffr., Theor. Gen. Crystallogr.*, 1977, **33**, 914–923.
23 C. B. Shoemaker, D. P. Shoemaker, T. Hopkins and S. Yindepit, *Acta Crystallogr., Sect. B: Struct. Crystallogr. Cryst. Chem.*, 1978, **34**, 3573–3576.
24 Z. L. Wang, Z. Dai and S. Sun, *Adv. Mater.*, 2000, **12**, 1944–1946.
25 N. Arora and B. R. Jagirdar, *J. Mater. Chem.*, 2012, **22**, 20671–20679.
26 D. Srikala, V. Singh, A. Banerjee, B. Mehta and S. Patnaik, *J. Phys. Chem. C*, 2008, **112**, 13882–13885.